Journal of Applied Polymer Science

Synthesis, Thermal Degradation, and Flame Retardancy of a Novel Charring Agent Aliphatic—Aromatic Polyamide for Intumescent Flame Retardant Polypropylene

Jiangsong Yi, Yi Liu, Dongdong Pan, Xufu Cai

Department of Polymer Science and Engineering, State Key Laboratory of Polymer Materials Engineering, Sichuan University, Chengdu 610065, People's Republic of China

Correspondence to: X. Cai (E-mail: Caixf2004@sina.com)

ABSTRACT: In this article, the laboratory-made poly(p-ethylene terephthalamide) (PETA) was used as a novel charring agent; it was characterized by Fourier transform infrared spectroscopy and ^{1}H NMR. PETA combined with ammonium polyphosphate (APP) to prepare the intumescent flame retardant (IFR), which was applied in polypropylene (PP). The flame retardancy of IFR on PP was investigated by the limiting oxygen index (LOI), the UL-94 (vertical flame) test, thermogravimetric analysis (TGA), and scanning electron microscopy (SEM). The results showed that the LOI value of the IFR-PP (30/70) system reached the highest 35%, and the system passed V-0 rating, when the weight ratio of PETA to APP was 1 : 3. The TGA data indicated that the charring ability of PETA was relatively poor with 18.0 wt % char residue at 800°C. However, the residual weight of the IFR was promoted with 28.1 wt % at 800°C, while it was 22.8 wt % based on calculation. The SEM showed that the intumescent and dense charring layer was formed after the combustion of the IFR-PP(30/70) system. In addition, the thermal degradation mechanism of PETA and IFR was studied by thermogravimetry-Fourier transform infraredspectroscopy and IR, and it demonstrated that the reaction between APP and PETA was happened and the P—O—C structure was got. © 2012 Wiley Periodicals, Inc. J. Appl. Polym. Sci. 000: 000–000, 2012

KEYWORDS: charring agent; intumescent flame retardant; synthesis; thermal degradation mechanism; polypropylene

Received 8 June 2011; accepted 16 April 2012; published online
DOI: 10.1002/app.37910

INTRODUCTION

Polypropylene (PP) is a large variety of common polymers; it is a widely used thermoplastic material because of its excellent mechanical properties, low density, good chemical resistance, and ease of processing. However, the use of PP in electric and electronic, building, or transport aspects is strongly limited because of their easy flammability with low limiting oxygen indices (LOI), which are of the order of 18%.[1] Thus, flame-retardant PP is urgently demanded. To improve the flame retardancy of PP and greatly meet the requirements of environmental protection, intumescent flame retardants (IFRs) are a growing group of halogen-free agents for flame retardant PP due to their advantages of little smoke and low toxicity during burning.[2–10] Particularly, they boost the flame retardancy of polyolefin effectively.

A general intumescent system includes acid catalyst, charring agent, and blowing agent. The mostly reported IFRs are the phosphorus–nitrogen containing compounds, and they give a uniform and swollen multicellular char on the surface of polymer, while burning; the charring layer act as a physical barrier against heat transmission, oxygen diffusion, smoke suppression, and dripping. The conventional acid catalysts are mainly phosphate and phosphate ester such as ammonium polyphosphate (APP), and the currently used charring agents are mainly small molecular compounds, e.g., pentaerythritol or dipentaerythritol. However, for small molecule charring agent, their thermal stability is relatively poor; in addition, their migration resistance and water resistance are unsatisfactory. Accordingly, the macromolecule with low water solubility and high charring ability is used instead of polyols to reduce or cancel above hazards to some extent.

The study of intumescent flame-retardant PP with APP as acid catalyst and polyamide (PA) as charring agent had been much reported,[11–18] and they exhibited good flame retardancy. However, aliphatic PA such as PA6, PA66 was easily melted during processing due to their low melting point, which resulted in the problem of poor compatibility between the charring agent and PP resin. Besides, the aromatic PA does not work during the

Applied Polymer SCIENCE

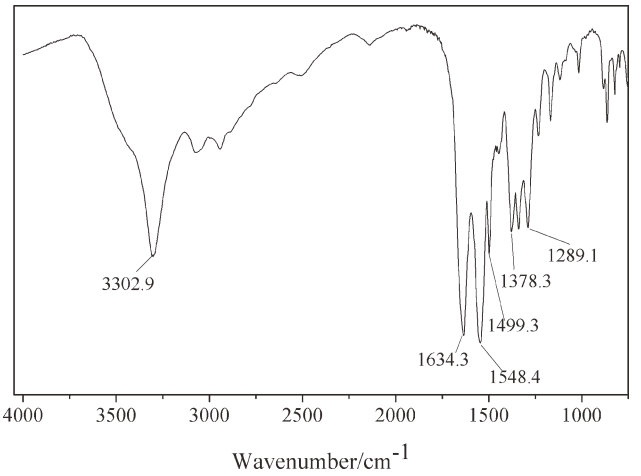

Figure 1. The FT-IR spectrum of PETA.

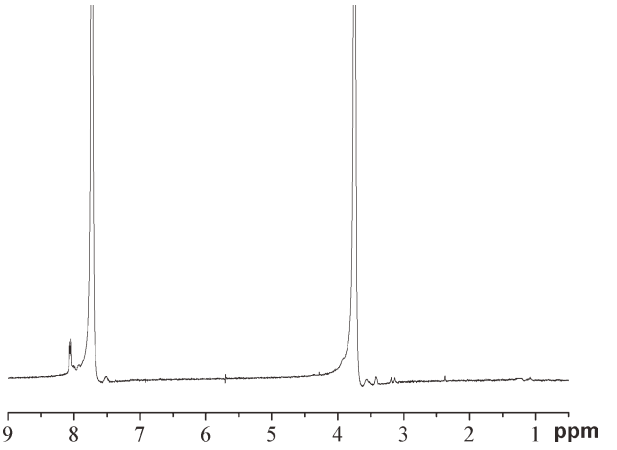

Figure 2. The ^{1}H NMR spectrum of PETA.

decomposition of matrix because of their high decomposition temperature. Based on this, a laboratory-made aliphatic–aromatic PA poly(p-ethylene terephthalamide) (PETA) was used as a charring agent in this article, coordinated with APP to prepare the IFR. The structure of PETA was analyzed by Fourier transform infrared spectroscopy (FTIR) and ^{1}H NMR. In addition, the effects of the novel charring agent on flame retardancy and thermal degradation of IFR-PP systems had been investigated by thermogravimetric analysis (TGA), thermogravimetry-Fourier transform infraredspectroscopy (TG-IR), and LOI tests.

EXPERIMENT

Material

PP resin (F401) used in this work was produced by Jilin Petrochemical (Jilin, China). APP (n > 5000) was supplied by Zhejiang Longyou GD Chemical Industry Corp. (Longyou, China). Terephthaloyl chloride (TPC), ethylenediamine, triethylamine (TEA), N-methyl pyrrolidone (NMP), and anhydrous lithium chloride (LiCl) were used to synthesize the PETA, and they were all purchased from Kelong Chemical Reagent Corp. (Chengdu, China). Concentrated sulfuric acid was got from Kelong Chemical Reagent Corp. (Chengdu, China).

Synthesis of PETA

LiCl (2.4 g) and NMP (200 mL) were fed into three-neck flask with a stirrer, and then ethylenediamine (0.1 mol) was added to the flask when LiCl completely dissolved, the system was cooled to around 0°C in a cryostat bath. The TPC (0.1 mol) was slowly added within about 0.5 h while stirring, then the system was allowed to further react at 35°C for 1 h, after that, TEA was added for neutralizing the HCl, the reaction stopped after 2 h. Successively, the reactant was poured into distilled water and then filtered. The white solid was washed by distilled water and dried in a vacuum at 100°C to constant weight (yield: 81.33%; $[\eta]$: 0.57).

Preparation of Flame-Retardant PP Samples

Well dried PETA, APP, and PP were mixed in a certain mass ratio; the mixture was extruded into pellets in a twin screw extruder (TSSJ–25, Chengguang, China) at a temperature range of 190–210°C. Then well dried pellets were added into the injection-molding machine (NISSAN PS40E5ASE, Tokyo, Japan) and molded into standard testing bars for further testing.

Methods

To characterize the structure of PETA, FTIR, and ^{1}H NMR were used. IR spectroscopy was applied with a Nicolet IS10 FTIR spectrometer (Nicolet Instrument, Madison, Wisconsin) with KBr pellets. ^{1}H NMR (400 Hz) spectra was recorded on a Varian INOVA-400 spectrometer (Varian Instrument, Palo Alto, California) with CF_3COOD as a solvent.

The intrinsic viscosity ($[\eta]$) was measured by Ubbelohde viscometer (Chengdu, China). The dried product (0.125 g) was dissolved in 25 mL concentrated sulfuric acid to obtain a transparent standard solution. Then, times of the standard solution and the pure concentrated sulfuric acid which flowed through the Ubbelohde viscometer were recorded as t_1 and t_0. The $[\eta]$ is calculated according to the formula as followed:

$$[\eta] = \frac{[2(\eta_{sp} - \ln \eta_r)]^{1/2}}{\rho}$$

Where $[\eta]$ is the intrinsic viscosity, dL/g, η_r is the relative viscosity, $\eta_r = t_1/t_0$, η_{sp} is the specific viscosity, $\eta_{sp} = \eta_r - 1$, ρ is the concentration of solution, g/L.

LOI data of all samples were obtained at room temperature with an oxygen index instrument (XYC-75) (Chengde Jinjian Analysis Instrument Factory, China) produced by Chengde Jinjian Analysis Instrument Factory, according to ASTM D2863-77 standard. The dimensions of all samples are 130 × 6.5 × 3

Scheme 1. Synthesis of PETA.

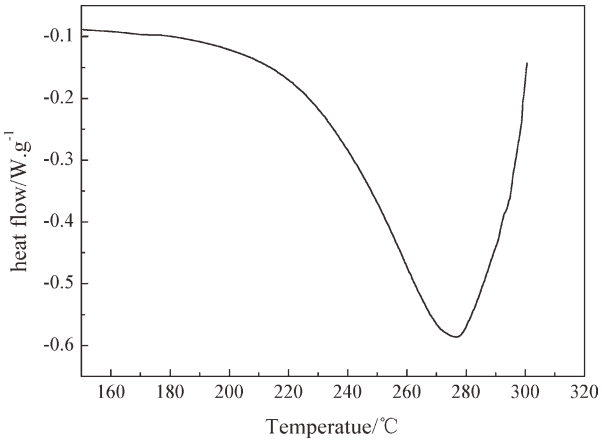

Figure 3. The DSC curve of PETA.

mm^3. Vertical burning rates of all samples were measured on a CZF-2 instrument (Jiangning Analysis Instrument Factory, China) produced by Jiangning Analysis Instrument Factory, with sample dimensions of 125 × 12.5 × 3.2 mm^3, according to UL-94 test (ASTM D635-77).

TGA was performed on a Mettler-Toledo instrument TGA/differential scanning calorimeter (DSC) 1 (Mettler-Toledo, Zurich, Switzerland) at a heating rate of 10°C/min. About 10 mg of the sample was examined under pure nitrogen or air condition at a flowing rate of 60 mL/min at temperatures ranging from 50 to 800°C.

TG-IR was performed using a SDT Q600 V20.5 Build 15 instrument that was interfaced to a Nicolet IS10 FTIR spectrometer. About 5.0 mg of the sample was put in an alumina crucible and heated from 50 to 800°C. The heating rate was set as 10°C/min (nitrogen atmosphere, flow rate of 60 mL/min).

The dried PETA powder was heated in DSC (mode: Q200, TA, American) from 50 to 300°C, the heating rate was set as 10°C/min.

The surface morphology of sample burning after the LOI test was observed and photographed in a Hitachi X-650 scanning electron microscope (SEM; Hitachi, Japan).

RESULT AND DISCUSSION

Characterization of PETA

The FTIR spectrum of PETA is given in Figure 1. Those very strong absorption peaks at 3302.9 cm^{-1} and 1548.4 cm^{-1} can be attributed to N—H stretching vibration and N—H blending vibration, respectively. The very strong absorption peak at 1634.3 cm^{-1} can be ascribed to C=O group on amido and the peak at 1289.1 cm^{-1} can be attributed to C—N stretching vibration. Those at 1499.3 cm^{-1} and 1378.3 cm^{-1} can be assigned to aromatic C=C stretching. Figure 2 presents the ^{1}H NMR spectrum of PETA in CF_3COOD. Peaks at 7.73 ppm and 3.74 ppm are due to aromatic protons and —CH_2— protons, respectively. The ratio of integration of H^a to that of H^b was 1 : 1. In addition, the peak at 8.06 ppm can probably be attributed to the N—H protons. Based on above discussions, the PETA was successfully synthesized, and the synthesis routes of PETA are shown in Scheme 1.

The DSC curve of PETA is given in Figure 3. As showed in Figure 3, we can clearly find that the melting point of PETA was 276°C. The melting point of PETA is higher than the process temperature.

Table I. The Flame Retardant Effect of IFR on IFR-PP Systems

Sample	PP/wt %	APP/wt %	PETA/wt %	LOI/%	UL-94
1#	100	-	-	18	No rating
2#	70	30	-	20	No rating
3#	70	-	30	21	No rating
4#	70	25	5	33	V-0
5#	70	24	6	34	V-0
6#	70	22.5	7.5	35	V-0
7#	70	20	10	31	V-0
8#	70	15	15	30	V-0
9#	75	18.75	6.5	29	No rating
10#	80	15	5	27	No rating
11#	82	13.5	4.5	26	No rating
12#	84	12	4	25	No rating
13#	90	7.5	2.5	23	No rating

Flame Retardancy

The PETA synthesized in this work was used as a novel charring agent, and it combined with APP, which used as an acid catalyst and a foaming agent, to prepare a new IFR. IFR was added to PP to obtain IFR-PP systems. Table I gives the flame retardant effect of IFR on IFR-PP systems. LOI and vertical burning rate (UL-94) are simple and important methods to evaluate the

Table II. Thermal Degradation Data by TGA

Sample	$T_{5\ wt\ \%}$[a]/°C	T_{1p}[b]/°C	R_{1pack}/°C^{-1}	T_{2p}[c]/°C	R_{2pack}/°C^{-1}
PP	289.4	372.4	4.35	-	-
APP	331.5	344	−8.25E-4	636	−0.0137
PETA	289	306.5	−0.00102	438	−0.0109
APP/PETA (3/1)	328	330.5	−0.00266	590	−0.00298
PP/APP (70/30)	315.7	430.6	−2.86	-	-
PP/PETA (70/30)	258.7	319.8	−11.4	546.5	−1.47
6#	319.5	423.9	−2.75	-	-

[a]the temperature of the 5 wt % weight loss, [b]the temperature of the first decomposition peak, [c]the temperature of the second decomposition peak.

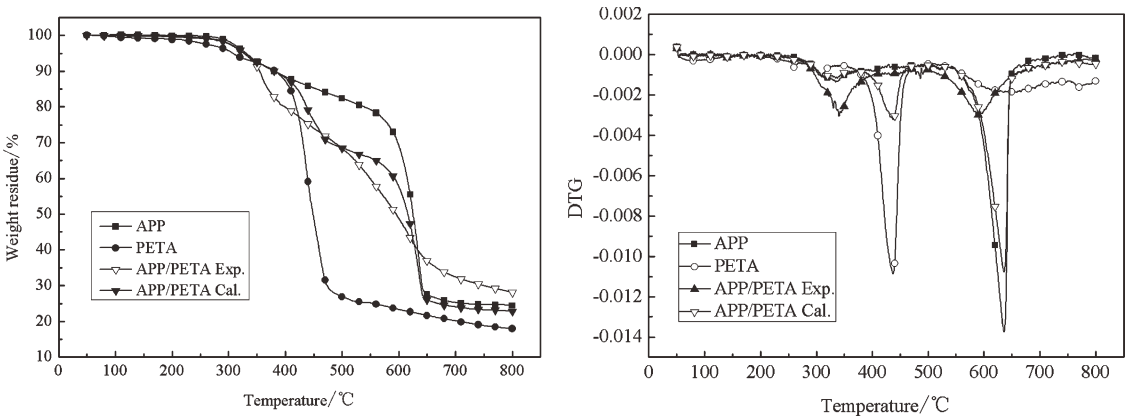

Figure 4. TG and DTG curves of APP-PETA system under pure nitrogen.

flame retardancy of polymeric materials. As shown in Table I, PP was easily flammable, accompanied with droplet, and its LOI value was only 18. It also could be seen that the alone addition of 30 wt % APP or 30 wt % PETA showed low flame-retardant efficiency on PP, LOI value of them was 20 and 21, separately. However, LOI values increased rapidly and exceeded 30 when APP and PETA were used together. The results in Table I also demonstrated that LOI value of IFR-PP systems increased with the increase of PETA. When the weight ratio of PETA to APP increased to 1 : 3, LOI value of IFR-PP system reached the best value (35). This formula of IFR demonstrated the best flame retardant efficiency on PP. However, when the ratio of PETA to APP continued to increase, LOI value of IFR-PP system decreased, the LOI decreased to 30 when the weight ratio of PETA to APP was 1 : 1. All of IFR-PP systems could reach V-0 rating in UL-94 test. Above all, this result proved that PETA combined with APP exhibited excellent flame retardancy. However, the LOI value of IFR-PP systems reduced rapidly with the decrease of the addition of IFR, and they were no rating in UL-94 test, when the addition of IFR was lower than 30%.

Thermal Degradation

Table II gives TGA data of the IFR and its components under pure nitrogen, and that of APP-PP, PETA-PP, and IFR-PP systems under air condition. Figure 4 shows TGA curves of APP, PETA, and APP/PETA systems under pure nitrogen. As shown in Table II and Figure 4, PETA was thermally stable below 280°C. Specifically, the thermal degradation process of PETA experienced two steps. In the first step, the decomposing temperature was between 280°C and 320°C, the main peak of thermal degradation was at 306.5°C. During this period, PETA mainly experienced chemical reactions of releasing carbon monoxide (CO) and carbon dioxide (CO_2) with the slow weight loss (about 8 wt % of the whole weight), proved by TG-IR. The second one occurred between 350°C and 510°C with a weight loss of 66 wt %, and the main peak of thermal degradation was at 438°C, the reaction of decomposition and crosslinking occurred during this period. Finally, the residual weight of PETA was 18.0 wt % at 800°C; this demonstrated that PETA had a relatively poor ability of charring by itself. The calculated curve in Figure 4 is the result by adding the curve of APP and that of PETA based on their percentages in APP/PETA system. According to Figure 4, the T_{1p} and T_{2p} of the APP/PETA system were reduced when they compared with the calculated data, and the experimental residual weight was lower than the calculated one when the temperature was below 630°C. In addition, we found that the main thermal degradation peak of APP/PETA at 590°C was earlier than that of APP and the calculated value in Figure 4, which showed that APP played a catalytic role in the degradation of PETA during the early period. However, the experimental residual weight of APP/PETA was higher than the calculated one, when the temperature was above 630°C. The residual weight of APP/PETA system at 800°C was 28.1 wt %, whereas it was 22.8 wt % based on the calculation. This demonstrated that APP changed the thermal degradation behavior of PETA and APP/PETA systems, and the char residue with highly thermal stability was obtained.

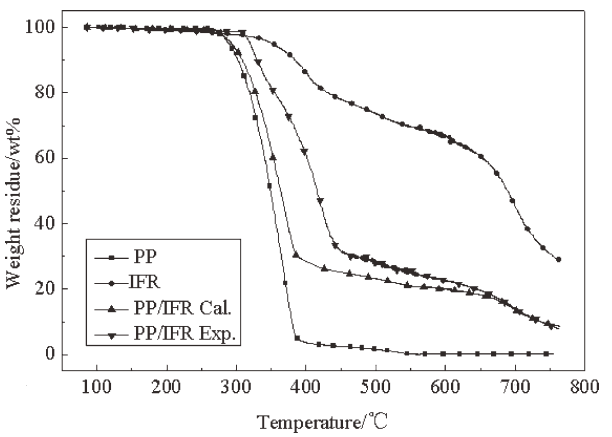

Figure 5. TG curves of IFR-PP system under air condition. IFR: APP/PETA = 3/1.

TGA curves of PP, IFR, and IFR-PP system under air condition are presented in Figure 5, and the thermal degradation data under air condition lists in Table II. IFR components are 75 wt % APP and 25 wt % PETA. The thermal degradation behavior of PP showed only one peak of PP backbone decomposition at 372.4°C. There was no residual weight remaining in PP over 400°C. From curves in Figure 5 and data in Table II, we found that IFR made a maximum peak of PP decomposition appear at

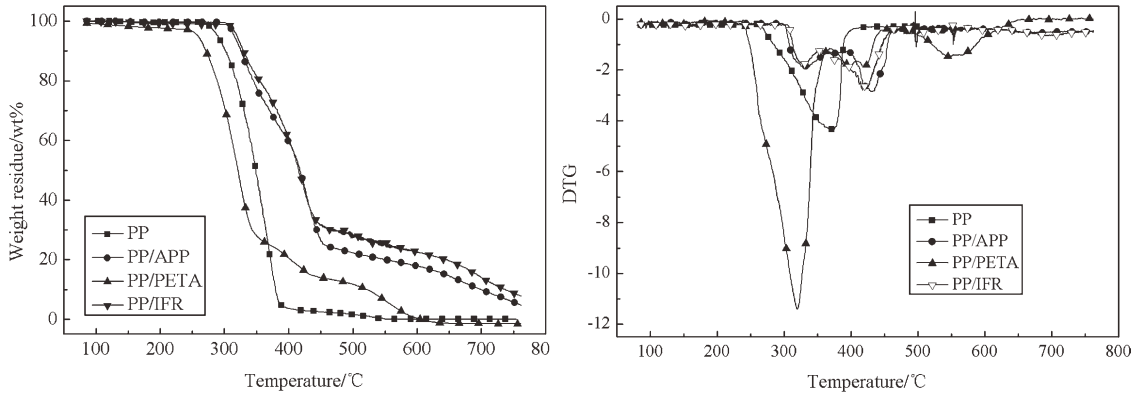

Figure 6. TG and DTG curves of PP, APP-PP, and PETA-PP and IFR-PP systems under air condition.

higher temperature (423.9°C). This was probably attributed to the fact that the interaction between APP and PETA occurred with the formation of a relatively stable carbide, which could prevent the under matrix from burning. However, when the temperature was above 650°C, the IFR-PP system experienced the second mass loss stage, it was due to the fact that the carbide began to collapse and degrade. The calculated curve in Figure 5 is based on curves of IFR and PP and their percentages in IFR-PP system. As shown in Figure 5, we found that the experimental residual weight of the IFR-PP system was higher than the calculated one at the temperature range of 300-650°C, while, with the increase of the temperature, the experimental residual weight of the IFR-PP system and the calculated one were basically equivalent, this phenomenon demonstrated that the interaction between IFR and PP was weak. Therefore, the main flame retardant mechanism was corresponded to the fact that the charring layer, generated by IFR, acted in condensed phase, which acted as a barrier to mass and heat, and the increase of the flame retardant efficiency of IFR on PP was not acquired by promoting the char formation ability of PP.

Figure 6 gives TGA curves and DTG curves of PP, APP-PP, PETA-PP, and IFR-PP systems under air condition, and the thermal degradation data under air condition lists in Table II. As shown in Figure 6 and Table II, APP and IFR made the maximum peak of PP decomposition appear at higher temperature, they took place at 430.6°C and 423.9°C, respectively. At the same time, PETA decreased the main decomposition peak and the $T_{5\ wt\ \%}$ of PETA-PP system, which appeared at 319.8°C and 258.7°C, respectively, and there was no residual weight remaining in the PETA-PP system over 600°C. It was probably due to the fact that the intermediate with isocyanate group was generated during the decomposition of PETA under high temperature, according to the thermal degradation mechanism of PETA, which was active and could accelerate the degradation of PP with the condition of high temperature and O_2. In addition, it demonstrated that the IFR-PP system possessed higher ability of charring than others, when the temperature was over 650°C. It could be explained that the charring layer formed by IFR had better thermal stability at high temperature.

TG-IR Test

TG-IR is a novel analytic technique to study the chemical structures and thermal decomposition mechanism of a polymer,[19–22] and it gives simultaneously a TGA curve and the IR spectrum of the gas from the TG system. In this work, TG-IR technique was used to characterize the volatilized products generated from the thermal degradation of PETA and APP/PETA (3/1).

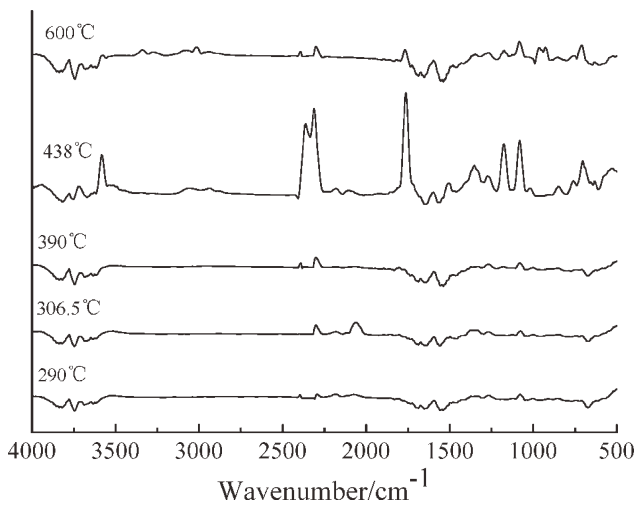

Figure 7. The FTIR spectra of volatilized products at various temperatures during the thermal degradation of PETA.

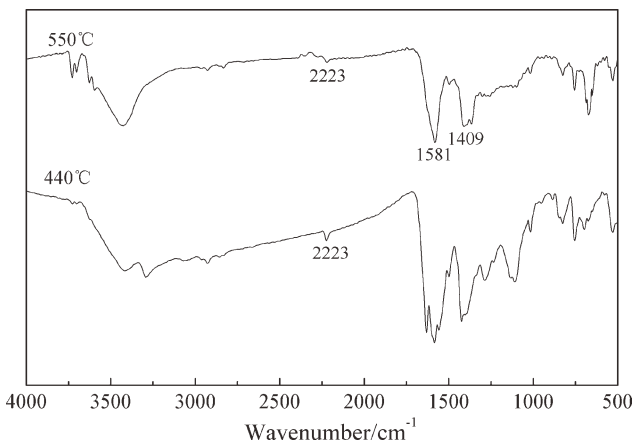

Figure 8. The FTIR spectrums of residual products at various temperatures during the thermal degradation of PETA.

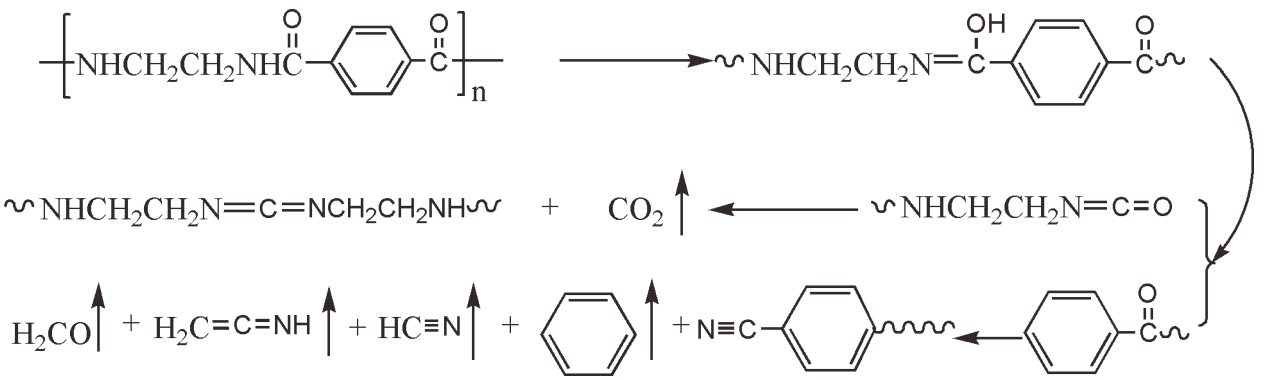

Scheme 2. The thermal degradation mechanism of PETA.

As shown in Figure 4, the PETA experienced two steps of decomposition, the first one at 280–320°C, the second one at 350–510°C. The stacked IR spectrums of gas escaping from the thermal degradation of PETA at different temperature are showed in Figure 7. As can be seen, a small amount of volatilized gases could be observed at 290°C. The volatilized product observed at 306.5°C can be identified as CO (characteristic peak at 2063 cm^{-1}) and carbon dioxide (characteristic peak at 2299 cm^{-1}). With the increase of temperature, the intensity of this characteristic peak of CO_2 increases, while that of CO decreases and disappears at 390°C. At higher temperature (about 438°C), the products are carbon dioxide (2361 cm^{-1}), formaldehyde (1763 cm^{-1}), HCN (2310 cm^{-1}), benzoate (1763 cm^{-1}, 1177 cm^{-1}, 1080 cm^{-1}), and the amido groups (3550 cm^{-1}).[23] The nitriles (HCN) formed at higher temperature are the result of dehydration of amides. Figure 8 gives the FTIR spectrums of residual products at various temperatures during the thermal degradation of PETA. At 440°C and higher temperature, the absorption peak at 2223 cm^{-1} can be ascribed to —C≡N group. At 550°C, those very strong absorption peaks at 1581 cm^{-1}, 1409 cm^{-1} can be attributed to stretching vibration of C=N in heat-resistant triazine ring, which was got from the trimerization of carbodiimide (—N=C=N—). Therefore, it turns out that the first breakpoint of PETA is located at the C—C bond near the benzene ring, and yields volatile products such as CO and CO_2, rather than locating at amido bond (—CO—NH—). The thermal degradation mechanism of PETA is showed in Scheme 2.

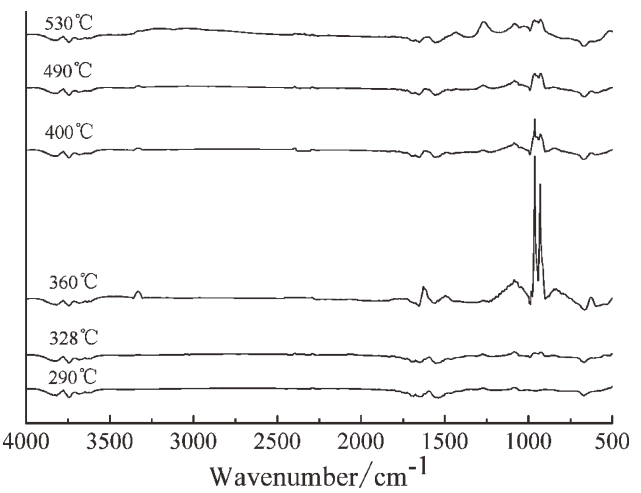

Figure 9. The FTIR spectra of volatilized products at various temperatures during the thermal degradation of APP/PETA.

Figure 9 represents the FTIR spectrums of volatilized products at various temperatures during the thermal degradation of APP/PETA (3/1). At 290°C, the IR spectrum of APP/PETA (3/1) is same with that of PETA. This demonstrates that only PETA starts to decompose at this temperature in the APP/PETA system. When the temperature increases to 328°C, APP begins to decompose, two sharp peaks at 964 cm^{-1} and 930 cm^{-1} and one peak at 3331 cm^{-1} are corresponding to the absorption of the ammonia,[24] and the intensity of this characteristic peak increases with the increase of temperature, reaching a maximum at 360°C. For temperatures at the range of 330–490°C, IR analysis shows that almost no other volatilized products exist. However, when the temperature is above 500°C, significant change occurs, there is a broad absorption at 3040 cm^{-1}, and two other peaks appear at 1597 cm^{-1} and 1433 cm^{-1}, these absorptions are attributed to gases containing benzene structure, the peak near 1267 cm^{-1} is assigned to the stretching vibration of P—O—C structure in phosphocarbonaceous (P—C) complex,[25] the peak near 1084 cm^{-1} corresponds to the P—O vibration in P—O—P groups.[26] Based on the above discussion, the reaction between APP and PETA was done. This may be due to the fact that the polyphosphoric acid, produced by the decomposition of the APP, catalyzes the degradation of PETA. Meanwhile, the polyphosphoric acid reacts with PETA to form the phosphate, which can prompt the char formation of the APP/PETA system by dehydration. Thus, the flame-retardant efficiency of IFR is improved.

Morphology of the Residual Char

To further investigate the effect of IFR on the char formation of the IFR-PP system during combustion, the morphology of chars was examined by SEM. SEM micrographs in Figure 10 show microstructures of the residues after LOI test. Figure 10(a) and (b) are char residue of the IFR-PP (30/70) system and that of the IFR-PP (25/75) system, respectively, the weight ratio of APP

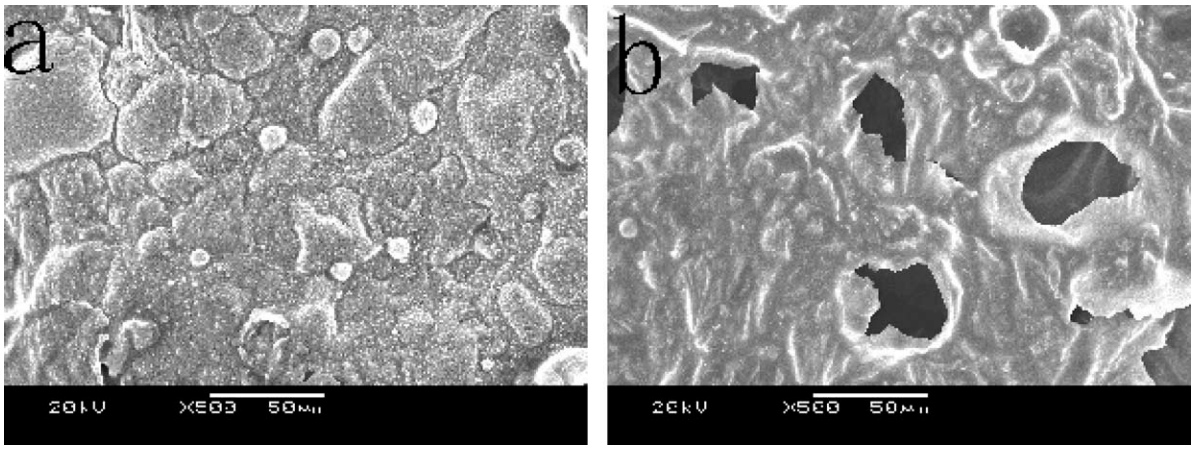

Figure 10. The SEM intumescent chars (×500): (a) IFR-PP (30/70), (b) IFR-PP (25/75).

to PETA is 3 : 1. For the IFR-PP (30/70) system, the surface of charring layer was compact, continuous and expansionary in Figure 10(a); at the same time, we could clearly find that the expansionary charring layer was not broke by the gas. It could separate the transfer of mass and heat between the gas and condensed phase. In addition, this kind of structure of the charring layer could offer a good shield to prevent melted PP from dripping and this had been proved in vertical flammability tests. However, the charring layer of the IFR-PP (25/75) system was expansionary but porous, there were many holes broken by the gas, and it could not form a continuous protective layer. Thus, the flame-retardant effect was poor, which was reflected in lower LOI value and no rating in UL-94 test.

CONCLUSIONS

With the single addition of APP or PETA, the flame-retardant efficiency on PP was low. However, when they use together, LOI values are significantly improved, and the optimum ratio of APP to PETA is 3 : 1, when the content of IFR is 30 wt %, LOI value of IFR-PP reaches 35 and V-0 rating is obtained in UL-94 test. TGA curves show that PETA has a relatively poor charring ability, however, when PETA combined with APP, there is an obvious synergistic effect between PETA and APP, which can enhance the char formation ability of IFR system. The residual weight of IFR under pure nitrogen reaches 28.1 wt % at 800°C while it is only 22.8 wt % based on calculation. However, the interaction between IFR and PP is weak, the residual weight of IFR-PP system is 19.6 wt % and the calculated one of IFR-PP system is 18.2 wt %, when the temperature was 650°C under air condition. The result from TG-IR demonstrates that APP changes the thermal degradation behavior of PETA and the reaction between APP and PETA is done. In addition, the morphology of chars investigated by SEM suggests that IFR-PP (30/70) can form a compact, continuous, and expansionary charring layer, which hinders effectively the transfer of heat and combustible gas and improves the flame retardancy and anti-dripping effects of PP.

ACKNOWLEDGMENTS

This work is financially supported by the National Natural Sciences Foundation of China, Grant NO. 50973066.

REFERENCES

1. Green, J. Flame-Retardant Polymeric Materials; Lewin, M.; Atlas, S. M.; Pearce, E. M., Eds.; Plenum Press: New York, **1982.**
2. Liu, Y.; Wang, D. Y.; Wang, J. S.; Song, Y. P.; Wang, Y. Z. *Polym. Adv. Technol.* **2008,** *19*, 1566.
3. Jang, B. N.; Jung, I.; Choi, J. *J. Appl. Polym. Sci.* **2009,** *112*, 2669.
4. Hoang, D. Q.; Kim, J.; Jang, B. N. *Polym. Degrad. Stab.* **2008,** *93*, 2042.
5. Lu, S. Y.; Hamerton, I. *Prog. Polym. Sci.* **2002,** *27*, 1661.
6. Camino, G.; Costa, L.; Martinasso, G. *Polym. Degrad. Stab.* **1989,** *23*, 359.
7. Ikuta, N.; Suzuki, Y.; Maekawa, Z.; Hamada, H. *Polymer* **1993,** *34*, 2445.
8. Hu, X.; Li, Y.; Wang, Y. Z. *Macromol. Mater. Eng.* **2004,** *289*, 208.
9. Ravadits, I.; Toth, A.; Marosi, G.; Marton, G.; Szep, A. *Polym. Degrad. Stab.* **2001,** *74*, 419.
10. Huang, H. H.; Tian, M.; Liu, L.; He, Z. H.; Chen, Z. Q.; Zhang, L. Q. *J. Appl. Polym. Sci.* **2006,** *99*, 3203.
11. Bourbigot, S.; Bras, M. L. *Macromol. Mater. Eng.* **2004,** *89*, 499.
12. Boubigot, S.; Bras, M. L.; Dabrowski, F. *Fire Mater.* **2000,** *24*, 201.
13. Almeras, X.; Bras, M. L.; Poutch, F. *Macromol. Symp.* **2003,** *198*, 435.
14. Almeras, X.; Renaut, N.; Jama, C. *J. Appl. Polym. Sci.* **2004,** *93*, 402.
15. Liu, Y.; Feng, Z.Q.; Wang, Q. *Polym. Compos.* **2009,** *30*, 221.
16. Ma, Z. L.; Zhang, W. Y.; Liu, X. Y. *J. Appl. Polym. Sci.* **2006,** *101*, 739.

17. Almeras, X.; Dabrowski, F.; Bras, M. L.; Poutch, F.; Boubigot, S.; Marosi, G.; Anna, P. *Polym. Degrad. Stab.* **2002,** *77*, 305.
18. Zhang, Y. X.; Liu, Y.; Wang, Q. *J. Appl. Polym. Sci.* **2010,** *116*, 45.
19. Devallencour, C.; Saiter, J. M.; Fafet, A.; Ubrich, E. *Thermochim. Acta.* **1995,** *259*, 143.
20. Pramoda, K. P.; Liu, T.; Liu, Z.; He, C.; Sue, H. *Polym. Degrad. Stab.* **2003,** *81*, 47.
21. Pramoda, K. P.; Liu, S. L.; Chung, T. S. *Macromol. Mater. Eng.* **2002,** *287*, 931.
22. Ratnam, C. T.; Nasir, M.; Baharin, A.; Laman, K. *J. Appl. Polym. Sci.* **2001,** *81*, 1914.
23. Zhang, Y.; Cheng, K. L.; Xu, J. R. *Thermochim. Acta.* **2005,** *425*, 137.
24. Riva, A.; Camino, G.; Fomperie, L.; Amigouët, P. *Polym. Degrad. Stab.* **2003,** *82*, 341.
25. Babrauskas, V. *Fire Mater.* **1995,** *19*, 243.
26. Wang, X. L.; Song, Y.; Bao, J. CH. *J. Vinyl Addit. Technol* **2008,** *14*, 120.